Article

Not peer-reviewed version

Path Following with Coaxial-Rotor MAV in the Presence of Wind Gusts

Arturo Tadeo Espinoza Fraire , José Armando Sáenz Esqueda * , Isaac Gandarilla Esparza , Jorge Alberto Orrante Sakanassi

Posted Date: 5 June 2025

doi: 10.20944/preprints202506.0452.v1

Keywords: coaxial-rotor MAV; linear control; nonlinear control

 doi:10.20944/preprints202506.0452.v1

Article

Path Following with Coaxial-Rotor MAV in the Presence of Wind Gusts

Arturo Tadeo Espinoza Fraire [1,†], José Armando Sáenz Esqueda [1,†,*], Isaac Gandarilla Esparza [1,†] and Jorge Alberto Orrante Sakanassi [2,†]

[1] Faculty of Engineering, Sciences and Architecture, Juarez University of the State of Durango, Gómez Palacio, Durango, México
[2] Instituto ecnologico de la Laguna, Departamento de Estudios de Posgrado e Investigacion, Torreón Coahuila, Mexico
* Correspondence: jsaenz@ujed.mx; Tel.:+52-8712-6408-05
† These authors contributed equally to this work.

Abstract: This work presents a nonlinear aerodynamic model that describes the dynamics of a coaxial-rotor MAV. We have designed seven control laws based on linear and nonlinear controllers for path following with a coaxial-rotor MAV in the presence of unknown disturbances, such as wind gusts. The linear controllers are the Proportional-Derivative (PD) and the Proportional-Integral-Derivative (PID). The nonlinear techniques are the nested saturation, sliding mode control, second-order sliding mode, high-order sliding mode, and adaptive backstepping. The results are presented after several computer simulations.

Keywords: coaxial-rotor MAV; linear control; nonlinear control

1. Introduction

The coaxial-rotor MAV (Mini Aerial Vehicle) is an unmanned aerial vehicle that has gained significant acceptance in the research area due to the compact structure of its components (fuselage, ailerons, motors, etc.). Another advantage is the wide variety of applications for these unmanned aerial systems. By the side of the research area with the coaxial-rotor MAV, focus is on design control laws, trajectory follow, aerodynamic structure research, materials analysis, etc. The before is necessary to realize applications in the real world as surveillance, target acquisition, area reconnaissance [1,2].

On the other hand, exists some disadvantages in the use of coaxial-rotor MAVs, some of them are that the design of the electronic systems should be small, and satisfy every necessity to achieve a stable flight. Another disadvantage is the aerodynamic structure design, for example, the distance between the top motor and the bottom motor must be sufficient but not too long to avoid the inter-rotor wash interference to obtain a fixed yaw angle and avoid the rotation in the z-axis in a hover flight.

Finally, these coaxial-rotor MAVs are subject to perturbations by wing gusts like other UAVs (Unmanned Aerial Vehicles). Then, there are a lot of areas of research about coaxial-rotor systems.

In the scientific literature is possible to find research about the coaxial-rotor UAVs to resolve some of the disadvantages mentioned before. For example in [3] is applied the fuzzy logic theory with sliding mode methodology to stabilize the longitudinal attitude of a small coaxial-rotor UAV, the control algorithm is designed decoupling the mathematical model of the coaxial-rotor UAV, with this controller design is possible suppress the modelling error and the external interference, the results of [3] are obtained by computer simulations. In [4] are combined the sliding mode control and PID control algorithm to stabilize the attitude of coaxial-rotor aircraft, the use of the two control laws combined is to achieve a steadily fly and keep the hover position, the mathematical model of the coaxial-rotor craft in [4], it is considering the blade element theory to calculated the brandishing motion of the blades, the results of sliding mode with PID control in [4] are presented in experiments. Other works are focused the research about the coaxial-rotor in the aerodynamics and the external forces acting in the coaxial-rotor UAV [5], and even proposed a better aerodynamic structure to carry generic payloads for

 doi:10.20944/preprints202506.0452.v1

different civil and agriculture applications, the results are presented in a numerical form by computer [5]. A combinatorial control method based on sliding mode coupled with a PID control is proposed in [6], and the dynamical model is divided in two subsystems, a fully-actuated subsystem and an under-actuated subsystem, the control objective is to control the position and attitude tracking of a coaxial-rotor aircraft, the results are presented in numerical simulations and experiments. In [7] is presented a $H\infty$ dynamic observer is presented to deal with the uncertainties and disturbance and design a control law to stabilize a ducted coaxial-rotor UAV.

It is presented in [8] a coaxial-rotor that it is designed to be small like a package and after to launch with other system, and even, it is development a complete nonlinear aerodynamic modelling for the coaxial-rotor UAV, but after it is simplified, the objective in [8], it is the application of a discrete Kalman filter to estimate the aerodynamic coefficients. In [9] is developed a compact coaxial-rotor to be launched with other propulsion system, and even the coaxial-rotor system includes a rotary-wing mechanism to achieve the rotations in roll and pitch angles, the control strategy is a cascade feedback controller, and in the first time was tested in a wind tunnel, and after tested from arbitrarily large attitude angles to demonstrate the control robustness.

In [10] it is presented a coaxial drone, adding in the aerodynamic structure two servo motors to control the roll and pitch angles, and it is developed a nonlinear dynamic model for the six degrees of freedom of the coaxial drone, and a nonlinear control allocation approach is proposed, the results are presented in numerical simulation, and validates in real experiments.

To achieve the control objective of trajectory tracking although the sensor noise, uncertainty in the model parameters, and external perturbations, in [11] it is proposed a nonlinear robust backstepping sliding mode controller to control the attitude and the position of a coaxial-rotor aircraft, the results are presented in numerical and flight experiments. By other side, in [12] it is proposed a control algorithm to stabilize the position and attitude of a coaxial-rotor drone, but without knowing the mathematical model dynamics, to achieve the objective of control in [12] it is proposed an optimal model-free fuzzy controller and estimating the unknown dynamic, the results are presented in numerical simulations.

In this work is develop a mathematical model dynamics that describes the coaxial-rotor MAV, this dynamic model includes the external disturbances by wind gusts, but in the controllers design is not considered such disturbances to analyze the control responses in the path following subject to unknown wind gusts and carry out a comparison between linear and nonlinear controllers. Then, the control laws that do not the known disturbances in this work are the linear controllers Proportional-Derivative (PD), the Proportional-Integral-Derivative (PID), and the nonlinear controllers based on nested saturation, the sliding modes methodologies based on first, second, and high-order.

It must be mentioned that we are proposing an adaptive backstepping control to try with these unknown disturbances, and to achieve a better path following with the coaxial-rotor MAV, and it is the only controller in this work that has considered the unknown disturbances to design an adaptation law based on the euler angles and angular rates for the roll and pitch angles, the before to eliminate or attenuate the unknown disturbances by wind gusts.

Then, this work is organized as follows: Section 2 shows the mathematical aerodynamic model to define the coaxial-rotor MAV; Section 3 presents the linear and nonlinear controllers design. Section 4 shows the simulation results obtained after several tests. Finally, Section 5 presents the discussion and the future work.

2. Coaxial-Rotor MAV Mathematical Model

In this section, it is presented the mathematical model that describes the coaxial-rotor MAV dynamics based on the Newton-Euler formulation [13–18]. The Earth's curvature is not considered due to the coaxial-rotor MAV flying short distances. To obtain the mathematical model, it is consider two coordinates frames $I_F = x_I, y_I, z_I$ and $B_F = x_B, y_B, z_B$ (see Figure 1), knowledge as the inertial fixed frame, and the body frame, respectively. The body frame is fixed, attached to the center of gravity

 doi:10.20944/preprints202506.0452.v1

of the coaxial-rotor MAV [19,20]. The general coordinates in the coaxial-rotor MAV are defined as $\overline{\mathbf{q}} = (x, y, z, \phi, \theta, \psi)^T \in \mathbb{R}^6$. The coaxial-rotor MAV mathematical model is given by:

$$\dot{\overline{\boldsymbol{\xi}}} = \overline{\mathbf{V}} \tag{1}$$

$$m\dot{\overline{\mathbf{V}}} = \Phi\mathbf{F} + \mathbf{F}_g \tag{2}$$

$$\dot{\boldsymbol{\eta}} = \boldsymbol{W}_{\eta}^{-1}\boldsymbol{\Omega} \tag{3}$$

$$\mathbb{I}\dot{\boldsymbol{\Omega}} = -\boldsymbol{\Omega} \times \mathbb{I}\boldsymbol{\Omega} + \boldsymbol{\Gamma} + k_* \boldsymbol{w}_* \tag{4}$$

with the translation coordinates relatives to the inertial frame $\overline{\boldsymbol{\xi}} = (x, y, z)^T \in \mathbb{R}^3$, $\mathbf{F}_g = (0, 0, mg)^T$ is the gravitational force. The translational velocity is defined by $\overline{\mathbf{V}} = (\dot{x}, \dot{y}, \dot{z})^T \in \mathbb{R}^3$ in B_F with respect to I_F. The mass of the coaxial-rotor MAV is represented by m. The forces working in the coaxial-rotor MAV are given by $\mathbf{F} = (F_x, F_y, F_z)^T \in \mathbb{R}^3$. The Euler angles are defined with $\boldsymbol{\eta} = (\phi, \theta, \psi)^T \in \mathbb{R}^3$, and $\boldsymbol{\Omega} = (p, q, r)^T \in \mathbb{R}^3$ is the angular velocity in B_F (see Figure 1). The torques working in the coaxial-rotor MAV are $\boldsymbol{\Gamma} = (\Gamma_L, \Gamma_M, \Gamma_N) \in \mathbb{R}^3)^T$ [21,22]. We have added to the aerodynamic model a unknown vector of the wind gusts perturbation $\boldsymbol{w}_* = (w_x, w_y, w_z)^T \in \mathbb{R}^3$, and $k_* > 0$ is applied to compensate the units of measurement. The inertial moments matrix is given by $\mathbb{I} \in \mathbb{R}^{3\times3}$. The matrix $\boldsymbol{W}_{\eta}^{-1}$ is defined as [23]

$$\boldsymbol{W}_{\eta}^{-1} = \begin{pmatrix} 1 & \tan\theta\sin\phi & \tan\theta\cos\phi \\ 0 & \cos\phi & -\sin\phi \\ 0 & \frac{\sin\phi}{\cos\theta} & \frac{\cos\phi}{\cos\theta} \end{pmatrix}$$

To obtain the orientation of the coaxial-rotor MAV is necessary to define a rotation matrix as $\Phi : B_F \to I \in SO(3)$:

$$\Phi = \begin{pmatrix} \cos\theta\cos\psi & \sin\phi\sin\theta\cos\psi - \cos\phi\sin\psi & \cos\phi\sin\theta\cos\psi + \sin\phi\sin\psi \\ \cos\theta\sin\psi & \sin\phi\sin\theta\sin\psi + \cos\phi\cos\psi & \cos\phi\sin\theta\sin\psi - \sin\phi\cos\psi \\ -\sin\theta & \sin\phi\cos\theta & \cos\phi\cos\theta \end{pmatrix}$$

Then, the Newton-Euler equations in a stable flight (hover flight) for a coaxial-rotor MAV are given by:

$$\ddot{x} = \frac{F_x}{m}c\theta c\psi + \frac{F_y}{m}(s\phi s\theta c\psi - c\phi s\psi) + \frac{F_z}{m}(c\phi s\theta c\psi + s\phi s\psi) \tag{5}$$

$$\ddot{y} = \frac{F_x}{m}c\theta s\psi + \frac{F_y}{m}(s\phi s\theta s\psi + c\phi c\psi) + \frac{F_z}{m}(c\phi s\theta s\psi - s\phi c\psi) \tag{6}$$

$$\ddot{z} = \frac{F_x}{m}s\theta + \frac{F_y}{m}s\phi c\theta + \frac{F_z}{m}c\phi c\theta - g \tag{7}$$

$$\ddot{\phi} = \frac{\dot{\theta}\dot{\psi}}{c\theta} + \frac{\dot{\theta}\dot{\phi}s\theta}{c\theta} + \frac{1}{I_{xx}}(\Gamma_L) + \frac{s\phi s\theta}{c_\theta I_{yy}}(\Gamma_M) + \frac{c\phi s\theta}{c\theta I_{zz}}(\Gamma_N) + \frac{k_* w_x}{I_{xx}} \tag{8}$$

$$\ddot{\theta} = -\dot{\theta}\dot{\phi}s\phi - \dot{\phi}\dot{\psi}c\theta + \frac{c\phi}{I_{yy}}(\Gamma_M) + \frac{\dot{\phi}}{I_{zz}}(-\Gamma_N) + \frac{k_* w_y}{I_{yy}} \tag{9}$$

$$\ddot{\psi} = \frac{\dot{\theta}\dot{\phi}}{c\theta} + \frac{\dot{\theta}\dot{\psi}s\theta}{c\theta} + \frac{s\phi}{c\theta I_{yy}}(\Gamma_M) + \frac{c\phi}{c\theta I_{zz}}(\Gamma_N) + \frac{k_* w_z}{I_{zz}} \tag{10}$$

with $c\phi = \cos\phi$, $c\theta = \cos\theta$, $c\psi = \cos\psi$, $s\phi = \sin\phi$, $s\theta = \sin\theta$, $s\psi = \sin\psi$.

$$\Gamma_L = \tau_\phi + q(I_{r1}\omega_{r1} - I_{r2}\omega_{r2}) + \overline{L} + qr(I_{yy} - I_{zz}) \tag{11}$$

$$\Gamma_M = \tau_\theta + p(-I_{r1}\omega_{r1} + I_{r2}\omega_{r2}) + \overline{M} - pr(I_{xx} - I_{zz}) \tag{12}$$

$$\Gamma_N = \tau_\psi + \overline{N} + pq(I_{xx} - I_{yy}) \tag{13}$$

 doi:10.20944/preprints202506.0452.v1

where I_{xx}, I_{yy}, I_{zz} are the inertial moments defined in the matrix $\mathbb{I} \in \mathbb{R}^{3\times3}$. The actuator moments are given by $\tau_\phi, \tau\theta, \tau\psi$ are the control inputs to generate the roll, pitch, and yaw angles, respectively. The angular velocities of the motors are defined with ω_{r1} and ω_{r2}, and the inertia moment of the propellers are given by I_{r1} and I_{r2}. Finally, the aerodynamic moments are $\overline{L}$ in roll angle, $\overline{M}$ in pitch angle, and $\overline{N}$ for yaw angle (see Figure 1).

2.1. Pitch Angle Response

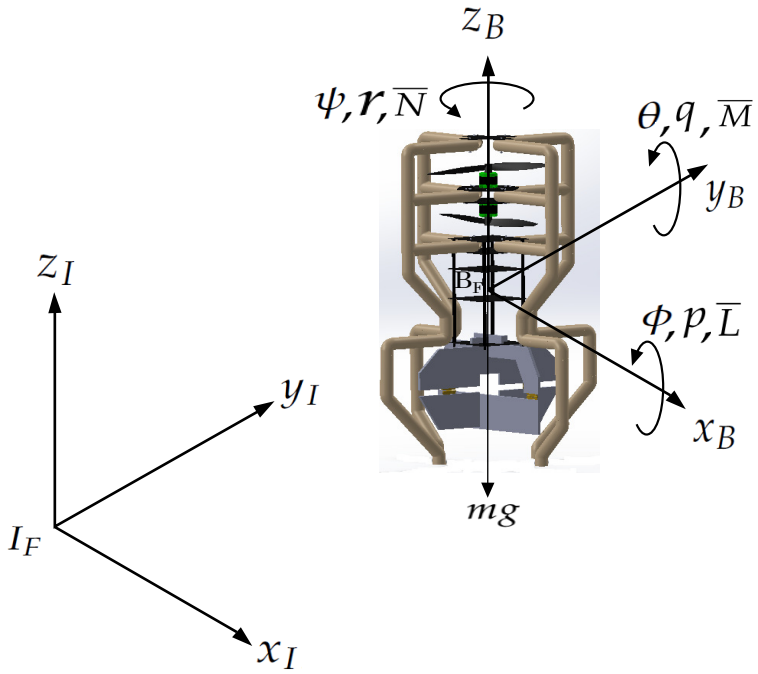

Figure 1. Coordinate systems on the coaxial-rotor MAV.

3. Linear and Nonlinear Controllers Design

To follow the desired trajectory with the coaxial-rotor MAV, in this work, the control laws are designed only for the pitch and roll angles; it is considered that the yaw angle is zero (the two brushless motors in the coaxial-rotor MAV work at the same speed). Then, to know which controller presents the better performance in the presence of unknown wind gust perturbations, let us decouple the equations (8)-(9) to obtain pure roll and pitch angles, but considering the unknown wind gust perturbations in the mathematical model. Thus, the equations to define a pure roll angle with perturbations are defined by:

$$\dot{\phi} = p \tag{14}$$

$$\dot{p} = \frac{\tau_\phi}{I_{xx}} + \frac{\bar{L}}{I_{xx}} + \frac{k_* w_x}{I_{xx}} \tag{15}$$

where $\bar{L} = \frac{1}{2}\rho V^2 S b C_l$, ρ is the air density, the velocity in hover flight is defined as V, the aileron area is defined with S, b is the aileron span, and C_l defined the aerodynamic coefficient in roll angle. The same procedure is considered to define the equations for a pure pitch angle with perturbations:

$$\dot{\theta} = q \tag{16}$$

$$\dot{q} = \frac{\tau_\theta}{I_{yy}} + \frac{\bar{M}}{I_{yy}} + \frac{k_* w_y}{I_{yy}} \tag{17}$$

 doi:10.20944/preprints202506.0452.v1

where $\bar{M} = \frac{1}{2}\rho V^2 S\bar{c}C_m$, $\bar{c}$ is the average aileron length, and C_m is the aerodynamic coefficient in pitch angle. The desired trajectory to follow by the coaxial-rotor MAV is defined as:

$$x_d = a_*[\text{atan}(\phi_d + \theta_d) + \text{atan}(t - \phi_d + \theta_d)]\cos(wt) \tag{18}$$

$$y_d = a_*[\text{atan}(\phi_d + \theta_d) + \text{atan}(t - \phi_d + \theta_d)]\sin(wt) \tag{19}$$

where x_d and y_d are the desired position in the x-axis and the y-axis, respectively. a_* is a positive constant value to define the circumference amplitude of the desired trajectory, t is the time, and w. ϕ_d, θ_d are the desired roll and pitch angle, respectively. To control the altitude of the coaxial-rotor MAV is design a PID controller defined by $u_z = m[g + \ddot{z}_p + k_{pz}(z_d - z) + k_{iz}\int(z_d - z)dt + k_{dz}(\dot{z}_d - \dot{z})]$, with $k_{pz}, k_{iz}, k_{dz} > 0$, z_d is the desired altitude, m is the total mass of the coaxial-rotor MAV, g is the gravitational constant.

It should be mentioned that is not considered in the control laws design, the unknown perturbation by wind gusts ($k_* w_*$) to compare the performance and robustness of the controllers in the presence of unknown perturbations. Except in the adaptive backstepping controller, it is proposed a wind gust estimation is proposed to eliminate or reduce the unknown perturbation defined in (14)-(17).

Thus, to design the linear controllers Proportional-Derivative (PD), and Proportional-Integral-Derivative (PID) for the roll angle, let us defined an error $e_\phi = \phi_d - \phi$, with ϕ_d as the desire roll angle, and ϕ defines the actual roll angle in the coaxial-rotor MAV. The PD control law for roll angle is given by [24,25]:

$$\tau_\phi = k_{p\phi}e_\phi + k_{d\phi}\dot{e}_\phi \tag{20}$$

where $k_{p\phi}, k_{d\phi} > 0$. The PID controller in pitch and roll angles for the coaxial-rotor MAV is defined as:

$$\tau_\phi = k_{p\phi}e_\phi + k_{i\phi}\int e_\phi dt + k_{d\phi}\dot{e}_\phi \tag{21}$$

with $k_{p\phi}, k_{i\phi}, k_{d\phi} > 0$. To design the nested saturation control in the roll angle, it is necessary to perform a linear transformation $z = T_{zx}x$ to transform the system (14)-(15) [26]:

$$\dot{z}_{1\phi} = z_{2\phi} \tag{22}$$

$$\dot{z}_{2\phi} = \frac{\tau_\phi}{I_{xx}} + \frac{\bar{L}}{I_{xx}} \tag{23}$$

Then,

$$\begin{bmatrix} z_{1\phi} \\ z_{2\phi} \end{bmatrix} = \begin{bmatrix} k_{2\phi}k_{1\phi} & k_{2\phi} \\ 0 & k_{1\phi} \end{bmatrix} \begin{bmatrix} x_{1\phi} \\ x_{2\phi} \end{bmatrix} \tag{24}$$

with $k_{2\phi}k_{1\phi} > 0$, $x_{1\phi} = \phi$ and $x_{2\phi} = p$. Let us define a saturation function $\sigma_a : \mathbb{R} \to \mathbb{R}$ with a limit a:

$$\sigma_a(s) = \begin{cases} -a, & s < -a \\ s, & -a \leq s \leq b \\ a, & s > a \end{cases} \tag{25}$$

where a is a constant positive value. Then, for the system (14)-(15) with the linear transformation (24) and the saturation function (25), the controller by nested saturation for roll angle to achieve global asymptotic stability is defined as:

$$\tau_\phi = -\sigma_2(z_{2\phi} + \sigma_1(z_{1\phi}))I_{xx} - \bar{L} \tag{26}$$

The first-order sliding mode control to stabilize the roll angle is defined from a sliding manifold $s_\phi = p + k_{1\phi}(\phi - \phi_d)$, and deriving the sliding manifold we have $\dot{s}_\phi = \frac{\tau_\phi}{I_{xx}} + \frac{\bar{L}}{I_{xx}} + k_{1\phi}(\phi - \phi_d)$. Then,

 doi:10.20944/preprints202506.0452.v1

to stabilize the roll angle defined with the system (14)-(15) using the first-order sliding mode control methodology [27], [28] is given by:

$$\tau_\phi = -\bar{L} + [-k_{1\phi}(\phi - \phi_d) - \beta_{1\phi}\,\text{sign}(s_\phi)]I_{xx} \tag{27}$$

where $k_{1\phi}, \beta_{1\phi} > 0$ are the controller gains, and the sign function is defined as:

$$\text{sign}(s_\phi) = \begin{cases} 1, & s_\phi > 0 \\ 0, & s_\phi = 0 \\ -1, & s_\phi < 0 \end{cases}$$

For the design of the second-order sliding mode is necessary a first-order robust differentiator, because a real-time derivative is sensitive to noise at the time of performing the derivative action. The robust real-time differentiator [29], and it is given by

$$\dot{x}_0 = v_0 = -\kappa_0|x_0 - s_\phi|^{1/2}\,\text{sign}(x_0 - s_\phi) + x_1 \tag{28}$$
$$\dot{x}_1 = -\kappa_1\,\text{sign}(x_1 - v_0) \tag{29}$$

with x_0 and x_1 are real-time estimates of s_ϕ and $\dot{s}_\phi$, respectively. The κ_0 and κ_1 are constant values to adjust the estimations. Then, to stabilize the roll angle with the second-order sliding modes [30], the controller obtained is:

$$\tau_\phi = -\bar{L} + [-k_{1\phi}(\phi - \phi_d) - \beta_{1\phi}\,\text{sign}(s_\phi) - \beta_{2\phi}\,\text{sign}(\dot{s}_\phi)]I_{xx} \tag{30}$$

where $k_{1\phi}, \beta_{1\phi}, \beta_{2\phi}$ are positive gains to adjust the second-order sliding mode controller. To design the high-order sliding mode, it is necessary to have a second-order robust differentiator [31], and it is given by:

$$\dot{x}_0 = v_0 = -\kappa_0|x_0 - s_\phi|^{2/3}\,\text{sign}(x_0 - s_\phi) + x_1 \tag{31}$$
$$\dot{x}_1 = v_1 = -\kappa_1|x_1 - s_\phi|^{1/2}\,\text{sign}(x_1 - v_0) + x_2 \tag{32}$$
$$\dot{x}_2 = -\kappa_2\,\text{sign}\,|x_2 - v_1| \tag{33}$$

where x_0, x_1, and x_2 are real-time estimations of s_ϕ, $\dot{s}_\phi$, and $\ddot{s}_\phi$. The constant values to adjust the estimations are defined by $\kappa_0, \kappa_1, \kappa_2$. Finally, the high-order sliding mode controller to stabilize the roll angle in the coaxial-rotor MAV is defined by:

$$\tau_\phi = -\bar{L} + [-k_{1\phi}(\phi - \phi_d) - \alpha_\phi(\ddot{s}_\phi + 2(|\dot{s}_\phi|^3 + |s_\phi|^2)^{1/6}\,\text{sign}(\dot{s}_\phi + |s_\phi|^{2/3}\,\text{sign}(s_\phi)))]I_{xx} \tag{34}$$

with $k_{1\phi}, \alpha_\phi$ as positive constant values. For the adaptive backstepping control in roll angle, we are considering the complete system (14)-(15), that is, we are consider the unknown perturbation $(\frac{k_* w_x}{I_{xx}})$ to design the adaptation law, and estimating w_x to reduced or eliminated the external perturbations in the coaxial-rotor MAV. Then, the error in roll angle is defined as $e_\phi = \phi - \phi_d$, and to begin with the adaptive control design, it is defined a Lyapunov candidate function is defined as:

$$V_{1\phi} = \frac{1}{2}e_{1\phi}^2 \tag{35}$$

Deriving (35):

$$\dot{V}_{1\phi} = e_{1\phi}\dot{e}_{1\phi} \tag{36}$$
$$= e_{1\phi}(q - \dot{\phi}_d) \tag{37}$$

 doi:10.20944/preprints202506.0452.v1

The new error is $z_{2\phi} = q - \alpha_{1\phi}$, where $\alpha_{1\phi} = \dot{\phi}_d - k_{1\phi}e_\phi$. Then, the derivative of (35) is $\dot{V}_{1\phi} = -k_{1\phi}e_\phi^2 + z_{2\phi}e_\phi$, due to the second term of the $\dot{V}_{1\phi}$ is not negative definite, and to continue with the design of the adaptive controller, we have to define a new Lyapunov candidate function given by:

$$V_{2\phi} = V_{1\phi} + \frac{1}{2}z_{2\phi}^2 + \frac{1}{2\gamma_{1\phi}}(k_* w_x - k_* \hat{w}_x)^2 \tag{38}$$

where $\gamma_{1\phi}$ are the adaptation gains, which are definite positive constants. Then, deriving (38):

$$\dot{V}_{2\phi} = \dot{V}_{1\phi} + z_{2\phi}\dot{z}_{2\phi} - (k_* w_x - k_* \hat{w}_x)\frac{\dot{\hat{w}}_x}{\gamma_{1\phi}} \tag{39}$$

Deriving the error $z_{2\phi} = q - \alpha_{1\phi}$:

$$\dot{z}_{2\phi} = \dot{q} - \dot{\alpha}_{1\phi} \tag{40}$$

$$\dot{z}_{2\phi} = \frac{\tau_\phi}{I_{xx}} + \frac{\bar{L}}{I_{xx}} + \frac{k_* w_x}{I_{xx}} - \ddot{\phi}_d + k_{1\phi}\dot{e}_\phi \tag{41}$$

Considering (39)-(41), the adaptive control law is given by:

$$\tau_\phi = -\bar{L} - k_* \hat{w}_x + (\ddot{\phi}_1^d - k_{1\phi}\dot{e}_\phi - e_\phi - k_2 z_{2\phi})I_{xx} \tag{42}$$

Thus,

$$\dot{V}_{2\phi} = -k_{1\phi}e_\phi^2 - k_{2\phi}z_{2\phi}^2 < 0 \tag{43}$$

with $k_{1\phi}, k_{2\phi} > 0$. The adaptation equation for the perturbations by wind gusts w_x is given by:

$$\dot{\hat{w}}_x = \frac{\gamma_{1\phi} z_{2\phi}}{I_{xx}} \tag{44}$$

The adaptation gain is defined by $\gamma_{1\phi}$. Finally, the equation (52) is negative definite, and it is considering bounded (53), it is possible to achieve definite global stability with the adaptive control law (51) for the system (14)-(15), which defines the roll angle in the coaxial-rotor MAV.

To control the pitch angle are used the same methodologies presented above are used, but applied to the system (16)-(17). Thus, the pitch error for pitch is given by $e_\theta = \theta_d - \theta$, with θ_d as the desired pitch angle, and θ defines the actual pitch angle. Thus, the linear controller PD and PID are given by:

$$\tau_\phi = k_{p\theta}e_\theta + k_{d\theta}\dot{e}_\theta \tag{45}$$

$$\tau_\theta = k_{p\theta}e_\theta + k_{i\theta}\int e_\theta dt + k_{d\theta}\dot{e}_\theta \tag{46}$$

where $k_{p\theta}, k_{i\theta}, k_{d\theta}$ are positive definite gains, In the appendix A and B are presented the stability proofs in the pitch angle for the PD and PID control laws, respectively. The nested saturation control for pitch angle is developed with the methodology presented in the equations (22)-(25). Thus, the nested saturation control to stabilize the pitch angle is given by:

$$\tau_\theta = -\sigma_2[z_{2\theta} + \sigma_1(z_{1\theta})]I_{yy} - \bar{M} \tag{47}$$

To achieve the desired pitch angle with the first-order sliding mode control (SMC), it is defined a sliding manifold is defined as $s_\theta = q + k_{1\theta}(\theta - \theta_d)$. Then, follow the methodology used for roll angle and SMC. The first-order sliding mode for pitch angle is defined as:

$$\tau_\theta = -\bar{M} + [-k_{1\theta}(\theta - \theta_d) - \beta_{1\theta}\,\mathrm{sign}(s_\theta)]I_{yy} \tag{48}$$

 doi:10.20944/preprints202506.0452.v1

where $k_{1\theta}, \beta_{1\theta}$ are positive values to tune in the controller. To design the second-order sliding mode is used the same structure of the robust differentiator (28)-(29) is used to obtain s_θ and $\dot{s}_\theta$, respectively. Thus, the second-order sliding mode control applied to the pitch angle is given by:

$$\tau_\theta = -\bar{M} + [-k_{1\theta}(\theta - \theta_d) - \beta_{1\theta}\,\text{sign}(s_\theta) - \beta_{2\theta}\,\text{sign}(\dot{s}_\theta)]I_{yy} \tag{49}$$

with the controller gains as $k_{1\theta}, \beta_{1\theta}, \beta_{2\theta} > 0$. Finally, to design the high order sliding mode controller to stabilize the pitch angle in the coaxial-rotor MAV is defined is used the same robust differentiator defined in (31)-(33) to obtain s_θ, $\dot{s}_\theta$, and $\ddot{s}_\theta$, respectively:

$$\tau_\theta = -\bar{M} + [-k_{1\theta}(\theta - \theta_d) - \alpha_\theta(\ddot{s}_\theta + 2(|\dot{s}_\theta|^3 + |s_\theta|^2)^{1/6}\,\text{sign}(\dot{s}_\theta + |s_\theta|^{2/3}\,\text{sign}(s_\theta)))]I_{yy} \tag{50}$$

where $k_{1\theta}, \alpha_\phi$ are positive constant. To design the adaptive backstepping law in pitch angle [32–34], it is necessary to follow the methodology presented from (35) to (53). Let us define the adaptive control law in pitch angle as:

$$\tau_\theta = -\bar{M} - k_*\hat{w}_y + (\ddot{\theta}_1^d - k_{1\theta}\dot{e}_\theta - e_\theta - k_2 z_{2\theta})I_{yy} \tag{51}$$

Then, the final derivative of the Lyapunov candidate function in pitch angle is:

$$\dot{V}_{2\theta} = -k_{1\theta}e_\theta^2 - k_{2\theta}z_{2\theta}^2 < 0 \tag{52}$$

where $k_{1\theta}, k_{2\theta}$ are positive definite gains to tune the adaptive controller. The adaptation equation for the perturbations by wing gusts w_y is given by:

$$\dot{\hat{w}}_y = \frac{\gamma_{1\theta} z_{2\theta}}{I_{yy}} \tag{53}$$

with $\gamma_{1\theta} > 0$ as the adaptation gain for the pitch angle.

4. Simulation Results

To do the comparison between the linear and nonlinear control laws, we have used the $\mathcal{L}_2 - norm$ to know the error of every controller applied to the coaxial-rotor MAV. The $\mathcal{L}_2 - norm$ for the error is defined as:

$$\mathcal{L}_2[e_s] = \sqrt{\frac{1}{T - t_0}\int_{t_0}^{T} \|e_s\|^2 dt} \tag{54}$$

The same *norm* is applied to calculate the control effort of each control law, and it is defined as:

$$\mathcal{L}_2[\tau_s] = \sqrt{\frac{1}{T - t_0}\int_{t_0}^{T} \|\tau_s\|^2 dt} \tag{55}$$

$s := \phi, \theta$ represents the roll and pitch angles in the coaxial-rotor MAV, respectively.

4.1. Roll Angle Response

The Figure 2, it is presented the roll angle response is presented with the different linear and nonlinear controllers. We can see oscillations due to the external perturbation (wind gusts). The PD, PID, and nested saturation controllers have presented more oscillations, but the perturbations in these control laws are oscillating on the desired roll angle to achieve the desired trajectory with the coaxial-rotor MAV. On the other hand, the nonlinear controllers based on sliding modes methodologies and adaptive backstepping have presented a better performance than PD, PID, and the nested saturation control in the presence of disturbances.

In the same Figure 2, it is appreciated that the sliding mode methodologies achieve the desired roll angle, but the second-order sliding mode (2SM) and high-order sliding mode (HOSM) achieve the desired roll angle with an overdamped signal form. On the other hand, we can see that the first-order

 doi:10.20944/preprints202506.0452.v1

sliding mode (SM) and the adaptive backstepping presented a critically damped signal form to achieve the desired roll angle.

The controller that presented a small error in roll angle is the adaptive backstepping, and the big error presented with the second-order sliding mode control (2SM), see Table 1.

Table 1. $\mathcal{L}_2 - norm$ error and control effort in roll angle

Roll Angle(ϕ)	$\mathcal{L}_2[e_\phi]$	$\mathcal{L}_2[u_\theta]$
PD	2.2186	1.6902
PID	2.1366	1.6902
Nested Saturation	1.9771	1.7372
Sliding Mode	2.9122	11.8892
Second-order Sliding Mode	4.9947	6.2838
High-Order Sliding Mode	4.4072	5.6993
Adaptive Backstepping	1.5271	1.7194

Analysing the control effort in the Table 1, the first-order sliding mode control (SM) presented a big control effort to achieve the control objective in the roll angle, and presented a bigger chattering effect in comparison with the second-sliding mode control (2SM), and the high-order sliding mode (HOSM), see the Figures 6–8. The PD and PID controllers applied a smaller control effort in comparison with the other control techniques in roll angle, but the adaptive backstepping is close to the control effort values presented with the PD and PID controllers, see Table 1.

The Figures 3 and 4 present the PD and PID control signals in the presence of the disturbances, respectively. The control signal responses for the nested saturation control and backstepping adaptive law are presented in Figure 5 and Figure 9, respectively.

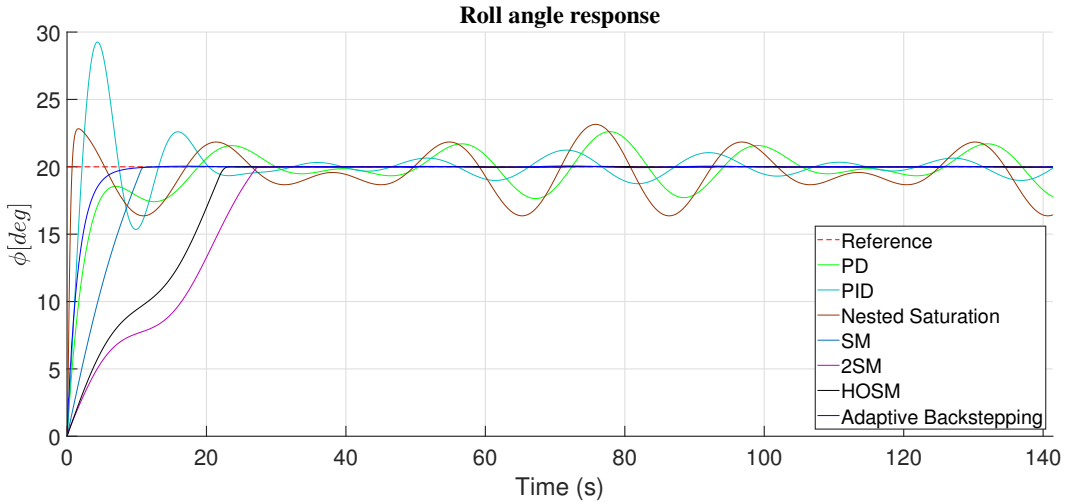

Figure 2. Response in roll angle (with disturbances).

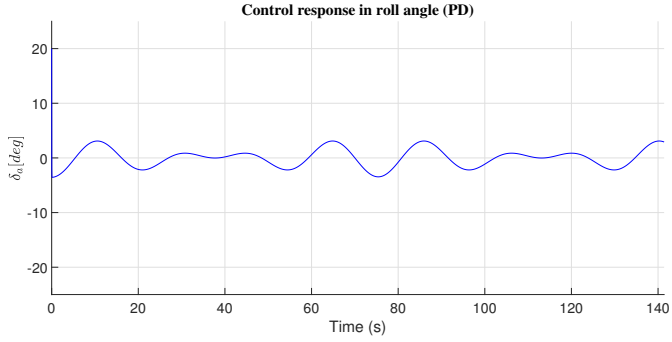

Figure 3. PD control response in roll angle (with disturbances).

 doi:10.20944/preprints202506.0452.v1

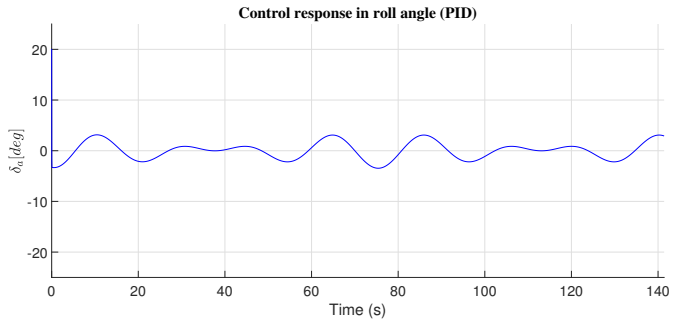

Figure 4. PID control response in roll angle (with disturbances).

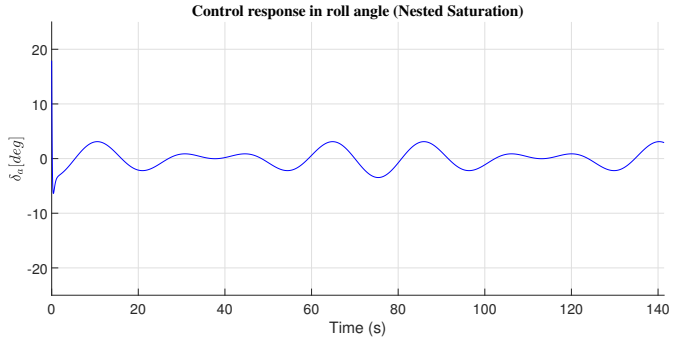

Figure 5. Nested saturation control response in roll angle (with disturbances).

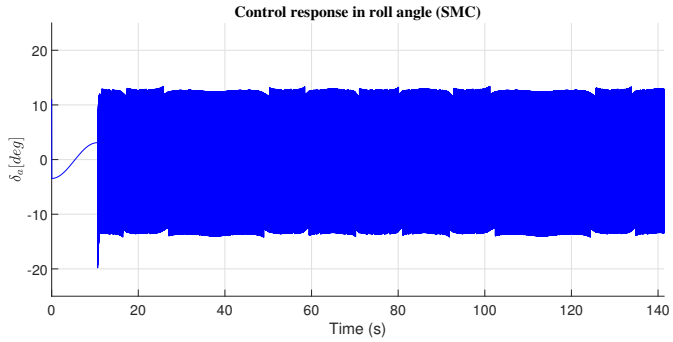

Figure 6. First-order sliding mode control response in roll angle (with disturbances).

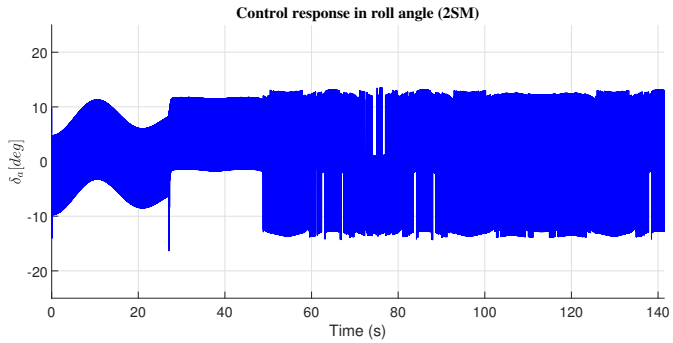

Figure 7. Second-order sliding mode control response in roll angle (with disturbances).

 doi:10.20944/preprints202506.0452.v1

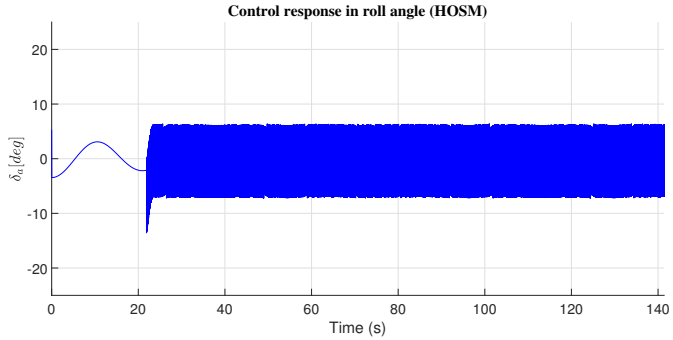

Figure 8. High-order sliding mode control response in roll angle (with disturbances).

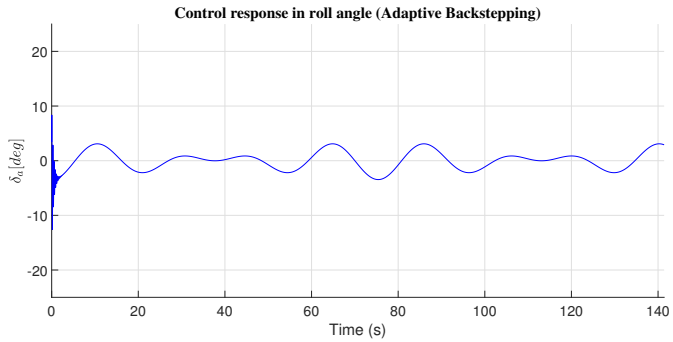

Figure 9. Adaptive backstepping control response in roll angle (with disturbances).

4.2. Pitch Angle Response

The pitch angle responses with the linear and nonlinear controllers are presented in Figure 10. The linear controllers PD and PID presented oscillations on the desired pitch angle, and the same signal is presented by the nested saturation control, which before due to the wind gusts. The second-order sliding mode (2SM) achieves the desired pitch angle as an overdamped signal. The first-order sliding mode control (SM), adaptive backstepping technique, and the high-order sliding mode (HOSM) achieve the desired pitch angle as a critically damped signal, see the Figure 10.

The control law with a small error presented in pitch angle is the adaptive backstepping, it can be appreciated in the Table 2. The big error in pitch angle is presented by the PD control.

Table 2. $\mathcal{L}_2 - norm$ error and control effort in pitch angle

Pitch Angle(θ)	$\mathcal{L}_2[e_\theta]$	$\mathcal{L}_2[u_\theta]$
PD	2.0078	1.6830
PID	2.6340	1.6826
Nested Saturation	1.2741	1.7097
Sliding Mode	0.9995	12.1660
Second-order Sliding Mode	1.5125	6.3147
High-Order Sliding Mode	1.3462	5.9203
Adaptive Backstepping	0.7598	1.6931

The PID control presented a small control effort to achieve the desired pitch angle, and the first-order sliding modes applied a big control effort to achieve the desired pitch angle, see the Table 2. Even more, in the Figures 14–16 it is appreciated that the first-order sliding mode control presented the biggest chattering effect in comparison with the second-order sliding mode (2SM) and high-order sliding mode (HOSM) controllers.

The Figure 11 and the Figure 12 present the control signal response in the presence of disturbances in the PD and PID controllers, respectively. The control signal for the nested saturation control and adaptive backstepping technique can be appreciated in the Figure 13 and Figure 17, respectively.

 doi:10.20944/preprints202506.0452.v1

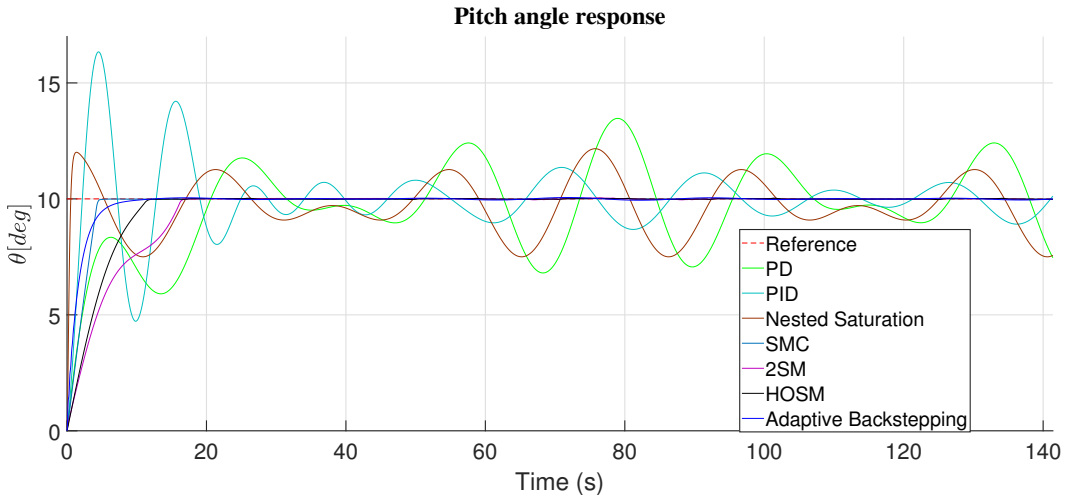

Figure 10. Response in pitch angle (with disturbances).

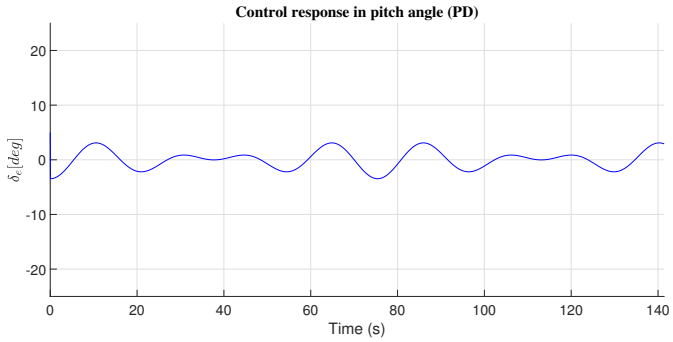

Figure 11. PD control response in pitch angle (with disturbances).

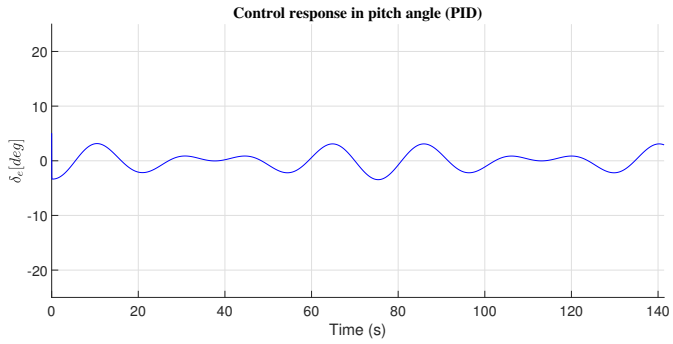

Figure 12. PID control response in pitch angle (with disturbances).

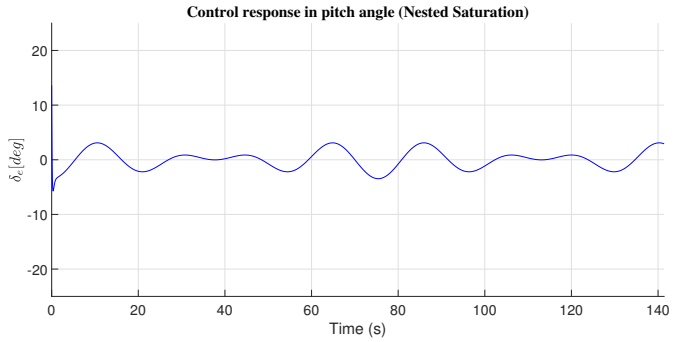

Figure 13. Nested saturation control response in pitch angle (with disturbances).

 doi:10.20944/preprints202506.0452.v1

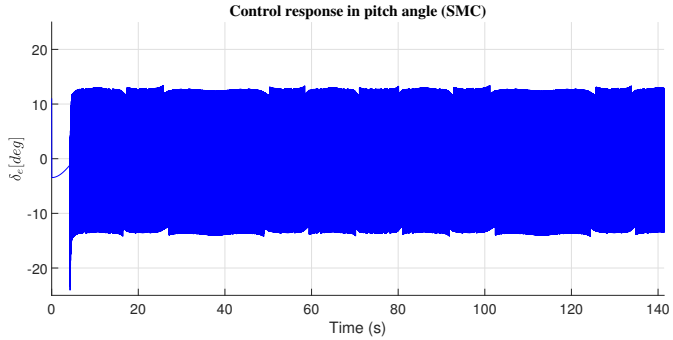

Figure 14. First-order sliding mode control response in pitch angle (with disturbances).

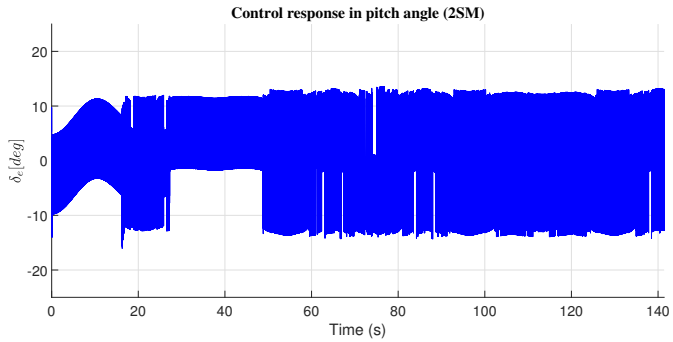

Figure 15. Second-order sliding mode control response in pitch angle (with disturbances).

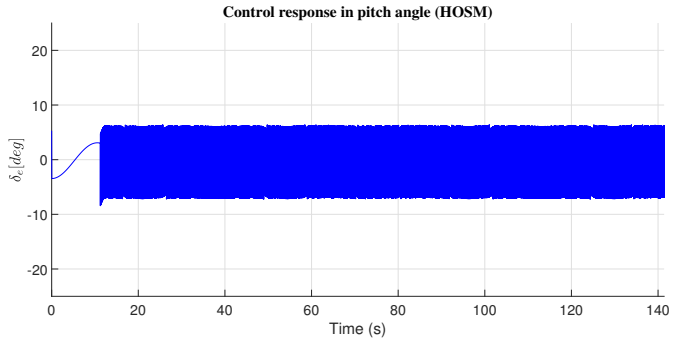

Figure 16. High-order sliding mode control response in pitch angle (with disturbances).

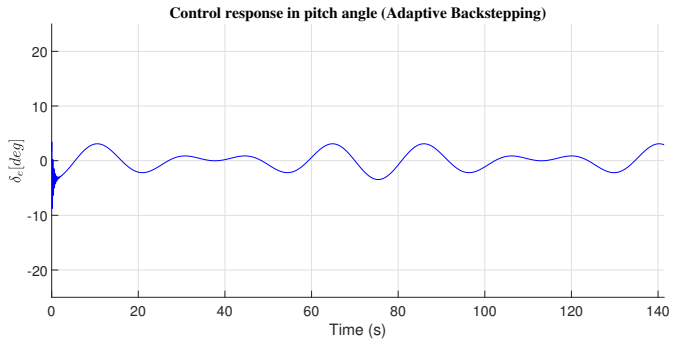

Figure 17. Adaptive backstepping control response in pitch angle (with disturbances).

4.3. Trajectory Follow by the Coaxial-Rotor MAV

In the Figures 18 and Figure 19 are presented the trajectory followed by the coaxial-rotor MAV and every linear and nonlinear controller in the x-axis and y-axis, respectively. The altitude is affected by the disturbances caused by wind gusts, the before can be seen in Figure 20. Finally, in the Figure 21, it is presented the complete trajectory to follow by the coaxial-rotor MAV.

 doi:10.20944/preprints202506.0452.v1

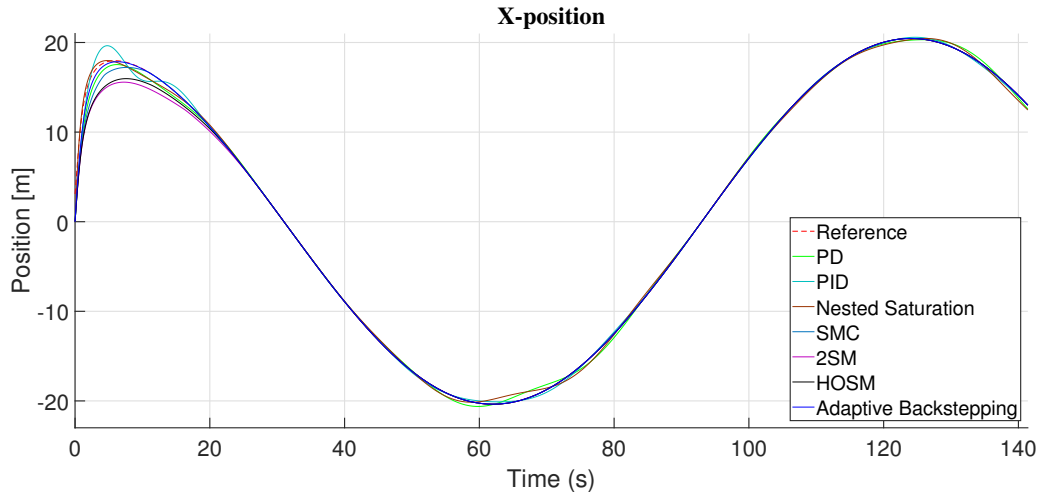

Figure 18. Controllers response in X-axis (with disturbances).

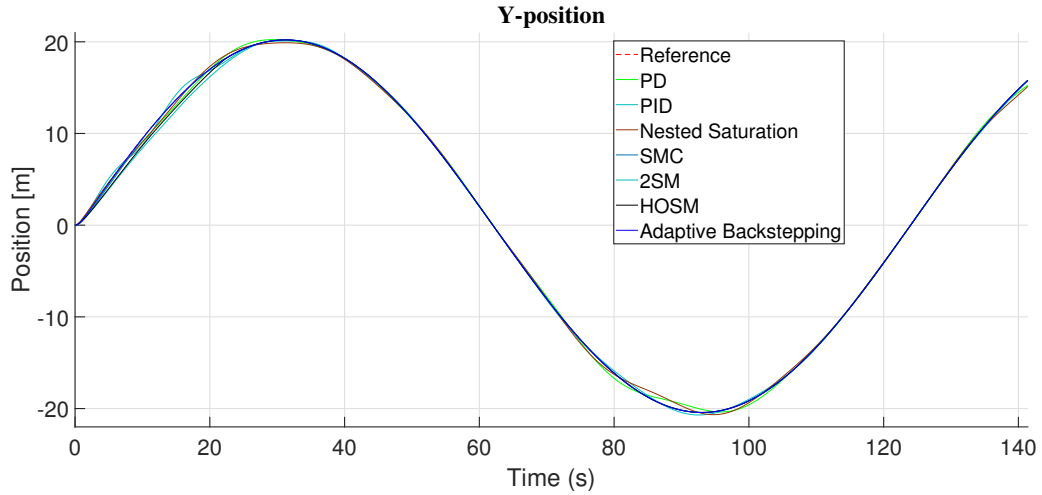

Figure 19. Controllers response in Y-axis (with disturbances).

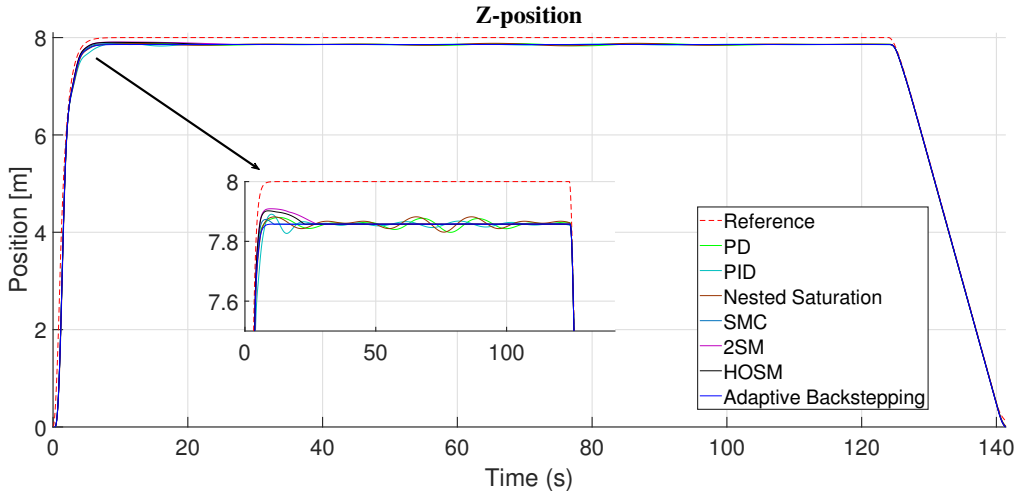

Figure 20. Controllers response in Z-axis (with disturbances).

 doi:10.20944/preprints202506.0452.v1

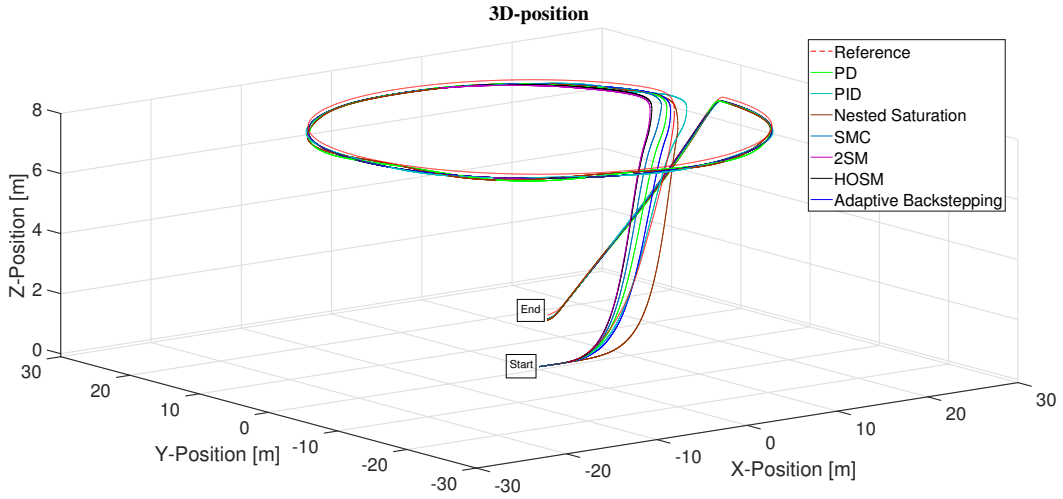

Figure 21. Trajectory in 3D (with disturbances).

5. Discussion

In this work it a comparison is presented between seven controllers in path following applied to a coaxial-rotor MAV, such control laws are linear and nonlinear control laws. The linear controllers are: Proportional-Derivative (PD) and Proportional-Integral-Derivative (PID). The nonlinear controllers are nested saturation, the sliding modes methodologies based on first, second, and high-order, and the adaptive backstepping technique.

The control laws were designed to path following through stabilizing the roll and pitch angles, the yaw angle, it is considered that the motors are working at the same velocity, in consequence the yaw angle is no changing during the path following, and the altitude control in the coaxial-rotor MAV was achieved with a PID control.

In roll angle, the PID control at the first twenty seconds presented an initial overshoot bigger than the nested saturation control and after twenty seconds persists some oscillations due to the disturbances by wind gusts, the PD control in roll angle presented oscillations too, but the nested saturation control presented a small oscillations in magnitude, in comparison with the PD and PID control (the same signal responses are obtained in the pitch angle). The three methodologies based on sliding modes in the roll angle achieved to desired roll angle in an overdamped signal form, and the controllers based on sliding mode presented an acceptable response in presence of the unknown disturbances, but the control signal has presented the undesired chattering effect, and the chattering effect was reduced but not eliminated by the high-order sliding mode control in the roll angle (it is presented the same effect in pitch angle).

The adaptive backstepping achieved to desired roll and pitch angles in a critically damped signal form, but remember that in these controllers an adaptation laws were designed to estimate the disturbances caused by wind gusts. The control laws that presented a smaller error in roll and pitch angles were the adaptive backstepping, and the bigger error in roll and pitch angles was presented by the second-order sliding mode and the PD, respectively. The smaller control effort in roll angle was presented by the PD and PID, but the smaller control effort signal in pitch angle was presented by the PID control, and the bigger control effort in roll and pitch angles was presented with the first-order sliding mode control.

In conclusion for this work the better response in path following with the coaxial-rotor MAV was achieved by the adaptive backstepping control, because the adaptive backstepping technique presented the smaller error for the control objective in roll and pitch angles, and even, the adaptive backstepping has applied only 1% more of control effort signal than the PD and PID controllers.

The future work consists of finishing the coaxial-rotor MAV to carry out experiments and probe in real flights the seven control laws developed in this work, and to demonstrate the stability proof for the nested saturation control and the sliding modes methodologies.

 doi:10.20944/preprints202506.0452.v1

Author Contributions: Conceptualization, T. and A.; methodology, T.; software, I.; validation, T., A. and I.; formal analysis, J.; investigation, T.; resources, I., and A.; data curation, A., and J.; writing—original draft preparation, T.; writing-review and editing, A., I.; visualization, A.; supervision, T., J.; project administration, T.; funding acquisition, T., A., and I. All authors have read and agreed to the published version of the manuscript.

Funding: Not applicable.

Institutional Review Board Statement: Not applicable.

Informed Consent Statement: Not applicable.

Data Availability Statement: Data available on request due to restrictions.

Conflicts of Interest: The authors declare no conflict of interest.

Abbreviations

The following abbreviations are used in this manuscript:

MAV	Mini Aerial Vehicle
DOF	Degrees of Freedom
SO(3)	Special Orthogonal Group in 3D
PD	Proportional-Derivative
PID	Proportional-Integral-Derivative
SMC	Sliding Mode Control
2SM	Second-order Sliding Mode
HOSM	High Order Sliding Mode

Appendix A

In this appendix is presented the PD stability proof in the pitch angle, the same methodology is used for the roll angle with PID controller, but in this work, it is only presented for pitch angle to avoid redundancies or repetitions in the writing. Be $\theta, \dot{\theta} \in \mathbb{R}$ the variable state of the pitch angle system. The dynamic of the system is defined as:

$$\frac{d}{dt}\begin{bmatrix}\theta \\ \dot{\theta}\end{bmatrix} = \begin{bmatrix}\dot{\theta} \\ \frac{1}{I_{yy}}(\tau_\theta + \bar{M})\end{bmatrix} \tag{A1}$$

where $I_{yy}, \bar{M} > 0$. Be $\theta_d \in \mathbb{R}$ the signal reference. It is defined the pitch angle error as:

$$e_\theta \triangleq \theta_d - \theta \tag{A2}$$

There is a control objective in the regulation such that:

$$\lim_{t\to\infty} e_\theta(t) = 0 \tag{A3}$$

For this purpose, the following control law is proposed.

$$\tau_\theta = k_{p\theta} e_\theta - k_{d\theta}\dot{\theta} \tag{A4}$$

where $k_{p\theta}, k_{d\theta} > 0$ is the proportional action gain and the derivative action gain, respectively.

Theorem A.1. *The system can be regulated* (A10) *for a value of* $\theta = \theta_d$*, by applying a control law in* (A4) *which guarantees global asymptotic stability with* $k_{p\theta}, k_{d\theta} > 0$*.*

 doi:10.20944/preprints202506.0452.v1

Proof. The system (A10) is rewritten in terms of the error e_θ as follows:

$$\frac{d}{dt}\begin{bmatrix} e_\theta \\ \dot{\theta} \end{bmatrix} = \begin{bmatrix} -\dot{\theta} \\ \frac{1}{I_{yy}}\left(k_{p\theta}e_\theta - k_{d\theta}\dot{\theta} + \bar{M}\right) \end{bmatrix} \tag{A5}$$

The closed loop system (A5) presents a single equilibrium point in $\theta = -\frac{\bar{M}}{k_{p\theta}}$, $\dot{\theta} = 0$. Since the equilibrium is located outside the origin, the following change of variable is proposed to move it to the origin:

$$\tilde{e}_\theta = e_\theta + \frac{\bar{M}}{k_{p\theta}} \tag{A6}$$

Substituting (A6) in (A5) Now the system can be written as:

$$\frac{d}{dt}\begin{bmatrix} \tilde{e}_\theta \\ \dot{\theta} \end{bmatrix} = \begin{bmatrix} -\theta \\ \frac{1}{I_{yy}}\left(k_{p\theta}\tilde{e}_\theta - k_{d_\theta}\dot{\theta}\right) \end{bmatrix} \tag{A7}$$

The equilibrium point of (A7) now it is $\tilde{e}_\theta = 0, \dot{\theta} = 0$. To demonstrate stability in the Lyapunov sense, the following candidate function is proposed, which is positive definite and radially unbounded:

$$V(\tilde{e}_\theta, \dot{\theta}) = \frac{1}{2}\frac{k_{p\theta}}{I_{yy}}\tilde{e}_\theta^2 + \frac{1}{2}\dot{\theta}^2 \tag{A8}$$

The derivative along the trajectories of (A8) is:

$$\begin{aligned} \dot{V}(\tilde{e}_\theta, \dot{\theta}) &= -\frac{k_{p\theta}}{I_{yy}}\tilde{e}_\theta\dot{\theta} + \dot{\theta}\ddot{\theta} \\ &= -\cancel{\frac{k_{p\theta}}{I_{yy}}\tilde{e}_\theta\dot{\theta}} + \cancel{\frac{k_{p\theta}}{I_{yy}}k_{p\theta}\tilde{e}_\theta\dot{\theta}}^{0} - \frac{k_{p\theta}}{I_{yy}}\dot{\theta}^2 \\ &= -\frac{k_{p\theta}}{I_{yy}}\dot{\theta}^2 \end{aligned} \tag{A9}$$

It can be observed that $\dot{V}(\tilde{e}_\theta, \dot{\theta}) \leq 0 \; \forall \; k_{p\theta}, k_{d\theta} > 0$. Having a positive definite and radially unbounded FCL, a derivative along the negative semidefinite trajectories, and the fact that the only equilibrium point is the origin, we can conclude the global asymptotic stability of the origin by employing the LaSalle Invariance Theorem. □

Appendix B

In this appendix is presented the PID stability proof in the pitch angle, the same methodology is used for the roll angle with PID controller, but in this work, it is only presented for pitch angle to avoid redundancies or repetitions in the writing. Be $\theta, \dot{\theta} \in \mathbb{R}$ the states of the system.

The system dynamic response is given by:

$$\frac{d}{dt}\begin{bmatrix} \theta \\ \dot{\theta} \end{bmatrix} = \begin{bmatrix} \dot{\theta} \\ \frac{1}{I_{yy}}(\tau_\theta + \bar{M}) \end{bmatrix} \tag{A10}$$

where $I_{yy}, \bar{M} > 0$. Be $\theta_d \in \mathbb{R}$ the reference signal, the error e_θ is defined as:

$$e_\theta \triangleq \theta_d - \theta \tag{A11}$$

 doi:10.20944/preprints202506.0452.v1

There is a control objective in the regulation such that:

$$\lim_{t\to\infty} e_\theta(t) = 0 \tag{A12}$$

For this purpose, the following control law is proposed.

$$\tau_\theta = k_{p\theta}e_\theta - k_{d\theta}\dot{\theta} + k_{i\theta}\int e_\theta dt \tag{A13}$$

where $k_{p\theta}, k_{d\theta}, k_{i\theta} > 0$ are the proportional, derivative and integral gains, respectively.

Theorem B.1. *The system can be regulated* (A10) *for a value of* $\theta = \theta_d$*, by applying a control law in* (A13) *which guarantees global asymptotic stability with* $k_{p\theta}, k_{d\theta}, k_{i\theta} > 0$.

Proof. The system (A10) is rewritten in terms of the error e_θ and $\omega \triangleq \int e_\theta dt$ as follows:

$$\frac{d}{dt}\begin{bmatrix}\omega\\ e_\theta\\ \dot{\theta}\end{bmatrix} = \begin{bmatrix} e_\theta \\ -\dot{\theta} \\ \frac{1}{I_{yy}}\left(k_{p\theta}e_\theta - k_{d\theta}\dot{\theta} + k_{i\theta}\omega + \bar{M}\right)\end{bmatrix} \tag{A14}$$

The closed loop system (A14) presents a single equilibrium point in $\omega = -\frac{\bar{M}}{k_{i\theta}}, e_\theta = 0, \dot{\theta} = 0$. Since the equilibrium is located outside the origin, the following change of variable is proposed to move it to the origin:

$$\tilde{\omega} \triangleq \omega + \frac{\bar{M}}{k_{i\theta}} \tag{A15}$$

Substituting (A15) in (A14) Now the system can be written as:

$$\frac{d}{dt}\begin{bmatrix}\tilde{\omega}\\ \tilde{e}_\theta\\ \dot{\theta}\end{bmatrix} = \begin{bmatrix} 0 & 1 & 0 \\ 0 & 0 & -1 \\ \frac{k_{i\theta}}{I_{yy}} & \frac{k_{p\theta}}{I_{yy}} & -\frac{k_{d\theta}}{I_{yy}}\end{bmatrix}\begin{bmatrix}\tilde{\omega}\\ e_\theta\\ \dot{\theta}\end{bmatrix} \tag{A16}$$

The equilibrium point of (A16) now is $\tilde{\omega} = 0$, $\bar{e}_\theta = 0$, $\dot{\theta} = 0$. To demonstrate stability, the direct Lyapunov method for linear systems will be used. The following Lyapunov candidate function is proposed:

$$V(\boldsymbol{x}) = \boldsymbol{x}^\top P \boldsymbol{x} \tag{A17}$$

with

$$\boldsymbol{x}^\top = \begin{bmatrix}\tilde{\omega} & e_\theta & \dot{q}\end{bmatrix} \tag{A18}$$

The matrix P It is symmetric and positive definite (i.e. $P = P\top > 0$) to ensure that the function is positively definite and radially unbounded. The derivative along the trajectories of (A17) is:

$$\begin{aligned}\dot{V}(\boldsymbol{x}) &= \dot{\boldsymbol{x}}^\top P\boldsymbol{x} + \boldsymbol{x}^\top P\dot{\boldsymbol{x}} && \text{(A19)}\\ &= \boldsymbol{x}^\top A^\top P\boldsymbol{x} + \boldsymbol{x}^\top PA\boldsymbol{x} && \text{(A20)}\\ &= \boldsymbol{x}^\top\left(A^\top P + PA\right)\boldsymbol{x} && \text{(A21)}\\ & && \text{(A22)}\end{aligned}$$

 doi:10.20944/preprints202506.0452.v1

where

$$A = \begin{bmatrix} 0 & 1 & 0 \\ 0 & 0 & -1 \\ \frac{k_{i\theta}}{I_{yy}} & \frac{k_{p\theta}}{I_{yy}} & -\frac{k_{d\theta}}{I_{yy}} \end{bmatrix} \tag{A23}$$

It is sought that $A^\top P + PA < 0$. Choosing P with the following form:

$$P = \begin{bmatrix} k_{i\theta} & p_{12} & p_{13} \\ p_{12} & k_{p\theta} & p_{23} \\ p_{13} & p_{23} & k_{d\theta} \end{bmatrix} \tag{A24}$$

and respecting the following dimensions for p_{12}, p_{13} and p_{23}:

$$p_{12}^2 < k_{p\theta} k_{i\theta} \tag{A25}$$

$$p_{13} < 0 \tag{A26}$$

$$p_{12} > \frac{p_{23}^2 k_{i\theta} + p_{13}^2 k_{p\theta}}{2 p_{13} p_{23}} \tag{A27}$$

An asymptotic stability of the origin can be guaranteed. □

References

1. Prior S.; Bell C. *Empirical Measurements of Small Aerial Co-Axial Rotor Systems*, Journal of Science and Innovation, Vol. 1, Issue. 1 pp. 1-18, 2011
2. Ramesh P.; Jeyan J. *Hover Performance Analysis of Coaxial Mini Unmanned Aerial Vehicle for Applications in Mountain Terrain*, Vilnius Gediminas Technical University-Aviation, Vol. 26, Issue. 2 pp. 1-12, 2022
3. Li K.; Wei Y.; Wang W.; Deng H. *Longitudinal Attitude Control Decoupling Algorithm Based on the Fuzzy Sliding Mode of a Coaxial-Rotor UAV*, MDPI Electronics, Vol. 8, Issue. 1 pp. 1-16, 2019
4. Wei Y.; Chen H.; Li K.; Deng H.; Li D. *Research on the Control Algorithm of Coaxial Rotor Aircraft based on Sliding Mode and PID*, MDPI Electronics, Vol. 8, Issue. 12 pp. 1-19, 2019
5. Singh V.; Kanani A.; Panchal N.; Mathur H. *Dynamic Analysis of Coaxial Rotor Systems*, International Journal of Mechanical and Production Engineering Research and Development, Vol. 10, Issue. 3 pp. 1-13, 2020
6. Wei Y.; Deng H.; Pan Z.; Li k.; Chen H. *Research on a Combinatorial Control Method for Coaxial Rotor Aircraft Based on Sliding Mode*, Elsevier Defence Technology, Vol. 18, pp. 280-292, 2022
7. Xu C.; Su C. *Dynamic Observer-based H-infinity Robust Control for a Ducted Coaxial-rotor UAV*, IET Control Theory and Applications, Vol. 16, pp. 1165-1181, 2022
8. Koehl A.; Rafaralahy H.; Boutayeb M.; Martinez B. *Aerodynamic Modelling and Experimental Identification of a Coaxial-Rotor UAV*, Journal of Intelligent and Robotic Systems, Vol. 68, pp. 53-68, 2020
9. Denton H.; Benedict M.; Kang H. *Design, development, and flight testing of a tube-launched coaxial-rotor based micro air vehicle*, International Journal of Micro Air Vehicles, Vol. 14, pp. 1-12, 2022
10. Chen L.; Xiao J.; Zheng Y.; Alagappan N.; Feroskhan M. *Design, Modeling, and Control of a Coaxial Drone*, IEEE Transactions on Robotics, Vol. 40, pp. 1650-1663, 2024
11. Xu J.; Hao Y.; Wang J.; Li L. *The Control Algorithm and Experimentation of Coaxial Rotor Aircraft Trajectory Tracking Based on Backstepping Sliding Mode*, MDPI Aerospace, Vol. 8, Issue. 11 pp. 1-17, 2021
12. Glida H.; Chelihi A.; Abdou L.; Sentouh C.; Perozzi G. *Trajectory Tracking Control of a Coaxial Rotor Drone: Time-delay Estimation-based Optimal Model-free Fuzzy Logic Approach*, ISA Transactions, Vol. 137, pp. 1-13, 2023
13. Goldstein H.; Poole C.; and Safko J. *Classical Mechanics*, Adison-Wesley, USA, 1983
14. Castillo P.; Lozano R.; Dzul A. *Modelling and Control of Mini-Flying Machines*, Ed. Springer, London, 2005
15. Garcia L.; Dzul A.; Lozano R.; Pégard A. *Quad Rotorcraft Control:Vision-Based Hovering and Navigation*, Ed. Springer-Verlag, London, 2013
16. O'Reilly O.M. *Intermediate Dynamics for Engineers*, Ed. Cambridge University Press, UK, 2020
17. Ardema M.D. *Newton-Euler Dynamics*, Ed. Springer, USA, 2005
18. Craig J.J. *Introduction to Robotics Mechanics and Control*, Ed. Pearson Education International, third edition, USA, 2005
19. Stengel R. F. *Flight Dynamics*, Princeton University Press, USA, 2004

 doi:10.20944/preprints202506.0452.v1

20. Cook M. *Flight Dynamics Principles*, Ed. Elsevier,Second edition, 2007
21. Stevens B.; Lewis F.; Johnson E. *Aircraft Control and Simulation*, Ed. Jhon Wiley and Sons, third edition, USA, 2015
22. Mclean D. *Automatic Flight Control Systems*, Ed. Prentice hall International, USA, 1990
23. Espinoza-Fraire T.; Dzul A.; Parada R.; Sáenz A. *Design of Control Laws and State Observers for Fixed-WIng UAVs: Simulation and Experimental Approaches*, Ed. Elsevier, UK, 2023
24. Kelly R.; Santibañez V.; Loría L. *Control of Robot Manipulators in Joint Space*, Ed. Springer, USA, 2005
25. Ogata K. *Modern Control Engineering*, Ed. Prentice Hall, Fifth edition, New Jersey, 2009
26. Teel A. *Global stabilization and restricted tracking for multiple integrators with bounded controls*, Systems and Control Letters, Vol. 18, Issue 3, pp. 165-171, 1992
27. Khalil H. *Nonlinear Systems*, Prentice Hall, third Edition, USA, 1995
28. Shtessel Y.; Edwards C.; Fridman L.; Levant A.; *Sliding Mode Control and Observation*, Birkhäuser, New York, 2015
29. Levant A. *Robust exact differentition via sliding mode technique*, Automatica, Vol. 34, Issue 3, pp. 379-384, 1998
30. Levant A. *Construction principles of 2-sliding mode design*, Automatica, Vol. 43, Issue 4, pp. 576-586, 2007
31. Levant A. *Higher-order sliding modes, differentiation and output-feedback control*, International Journal of Control, Vol. 76, Issue 9-10, pp. 924-941 , 2003
32. Åström K.; Wittenmark B. *Adaptive Control*, Ed. Prentice Hall, 2nd Edition, 1994
33. Kristić M.; Kanellakopoulos I.; Kokotović P. *Nonlinear and Adaptive Control Design*, Ed. John Wiley and Sons, USA, 1995
34. Wang W.; Wen C.; Zhou J. *Adaptive Backstepping Control of Uncertain Systems with Actuator Failures, Subsystem Interactions, and Nonsmooth Nonlinearities*, Ed. CRC Press, UK, 2017